J Electroceram (2011) 27:126–133
DOI 10.1007/s10832-011-9657-4

Preparation and characteristics of fine-grained ferroelectric glass-ceramic composites via a modified hybrid route at low temperature sintering

Hong-fang Zhang · Chee-leung Mak

Received: 31 May 2011 / Accepted: 9 September 2011 / Published online: 12 October 2011

Abstract Dense, homogeneous and fully developed fine-grained ferroelectric $Pb(Zr_{0.53}Ti_{0.47})O_3$–based glass-ceramics have been successfully prepared at a low-sintering temperature of 850–900°C by a modified hybrid process in air. The influence of the $PbO\text{-}B_2O_3\text{-}SiO_2$ (abbreviated as PBS) glass-gel content on the microstructure, dielectric, and ferroelectric properties of such glass-ceramics has been investigated. The temperature dependence of the dielectric constant indicated that the fine-grained $Pb(Zr_{0.53}Ti_{0.47})O_3$ (abbreviated as PZT(53/47)) based glass-ceramic shows the characteristic dispersion at the Curie point. Ferroelectric hysteresis loop analyses have been performed to manifest the ferroelectric nature of the highly crystallized PZT(53/47) phase prepared by this modified novel hybrid process despite containing higher wt% glass-gel contents. The best dielectric and ferroelectric properties in a typical sample with 5% by weight of glass-gel content were found to have dielectric constant and loss tangent of 920 and 0.02 at 1 kHz, respectively. The saturation polarization (P_s), and remanent polarization (P_r) as well as the coercive field (E_c) are 21.9 μC/cm^2, 10.8 μC/cm^2 and 2.19 kV/mm, respectively.

H.-f. Zhang
Department of Physics,
Suzhou University of Science and Technology,
Suzhou 215009, China
e-mail: zhf057@gmail.com

H.-f. Zhang · C.-l. Mak (✉)
Department of Applied Physics,
The Hong Kong Polytechnic University,
Hung Hom Kowloon, Hong Kong
e-mail: apaclmak@polyu.edu.hk

Keywords Characterization · Modified hybrid process · Finer glass-ceramic composites · Ferroelectric materials

1 Introduction

Low temperature sintering is always the trend in commercial production of electronic ceramics, especially for multi-layer device. $Pb(Zr,Ti)O_3$ (PZT) based thick film and multilayer components are being increasingly used owing to the simultaneous requirements of device miniaturization, lower operating voltages and devices integration [1–6]. PZT with composition near the morphotropic phase boundary (MPB) is the most widely used and studied piezoelectric ceramic to date, due to its high piezoelectric coefficient and high Curie temperature [7]. Normally, PZT which is prepared via conventional solid-state reaction between their constituent oxides is sintered at temperatures between 1200 and 1300°C. However, presence of intermediate reactions between these oxides results in compositional fluctuations and secondary phases [8]. Therefore, it is desirable to lower the sintering temperatures for multi-layer components and thick-film devices as low co-firing temperature enables the use of cheaper internal electrodes with lower melting point. Also, low sintering temperature reduces energy consumption and PbO evaporation during the fabrication process. Indeed, an uncontrolled loss of PbO results in deteriorated electrical properties and is furthermore an environmental concern [9].

A lot of effort has been spent for over 30 years to reduce the sintering temperature of PZT while retaining good piezoelectric characteristics [10–12]. Importantly, ferroelectric glass-ceramics with a fine-grain structure have attracted much attention and exhibited potential in many important applications such as piezoelectric sensors and actuators [13–15]. In general, glass-ceramics with high-crystalline

phase content are desirable for better dielectric properties; however, the content is quite limited by using the conventional glass-ceramics technique via a melting/quenching process. It is understandable that fine-grained PZT glass-ceramics with a substantial amount of pure PZT crystalline phase are difficult to fabricate via conventional melting because of the high volatility of the lead composition and the high melting temperature of the zirconium composition. Furthermore, the crystallization kinetics and phase development are difficult to control when going from a completely amorphous state. Besides, zirconium is simply not soluble in many types of glass. On the other hand, ferroelectric glass-ceramics derived from conventional sol–gel process, such as $BaTiO_3$–B_2O_3–SiO_2, $PbTiO_3$–B_2O_3–SiO_2, $PbTiO_3$–PbO–B_2O_3–SiO_2, Pb(Zr,Ti)O_3–B_2O_3–SiO_2 and Pb(Zr,Ti)O_3–PbO–B_2O_3–SiO_2 systems [16–19], were reported to have the possibility of obtaining dense and fine ceramics. However, the drawback of sol–gel method is the problems existed in processing fine/ultrafine powders with ceramics. Both the aggregation of ultrafine powders and formation of secondary phases are still difficult to be overcome by sol–gel processing, hence their physical properties are inferior to their counterpart [20].

In order to bridge the gap between these two processes, a hybrid process has been described in our previous reports [21–23]. By dispersing nano-sized crystalline particles obtained from a conventional solid state reaction into a sol–gel matrix (i.e. the precursor sol solutions as matrix), this hybrid process provides a promising processing to get a dense, well-crystallized and fine-grained ferroelectric glass-ceramic at relatively low sintering temperature. The key characteristic of this hybrid technology is to graft the sol–gel wet chemistry process into the conventional mixed oxide ceramic process. The high performance of the ceramics prepared by conventional ceramic process under high temperatures can be mostly preserved, while the sintering temperature of the material can be effectively reduced down as inherited from the sol–gel process. In this work, we propose an improved hybrid process by using the nano-crystalline composite technique to realize well-sintered, and fine-grained ferroelectric glass-ceramics prepared at low temperature sintering. In this modified hybrid process route, the nano-sized $Pb(Zr_{0.53}Ti_{0.47})O_3$ particles were dispersed uniformly in the glass PBS gel-solution, instead of the sol precursor solution as the matrix, and sintered at temperatures of 850–900°C. A dense, homogeneous, and fine-grained ferroelectric glass-ceramic composite were achieved successfully. This new modified hybrid technique provides an easy, flexible and reproducible process, and can be extensively used in screen-printing, tape-casting or even in traditional ceramic process to reduce the processing temperature. The synthesis, microstructures, dielectric, and ferroelectric properties of the glass-ceramic composites were investigated in more details in the following sections.

2 Experimental

2.1 Synthesis of nano-sized PZT(53/47) powders, uniformly distributed PZT(53/47)-glass slurry, and glass-ceramic composites

Nano-sized PZT(53/47) powders were prepared via a polymer-assisted (polyvinylpyrrolidone, PVP-K30 with number-average molecular weight of 10,000) sol–gel method [24]. A light yellowish transparent solution was formed by adjusting the PZT(53/47) sol precursor concentration to be 0.4 M. The PZT (53/47) precursor was then dried at 120°C for 10 h, resulting in a dried gel-PVP precursor. The nano-sized PZT powders were obtained by annealing the dried gel-PVP precursor at 800°C for 2 h. For the glass-ceramics, net-work forming oxides must be chosen properly to minimize interactions between the constituents of the glass and the desired crystalline phase [25]. In the present investigation, PbO-B_2O_3-SiO_2 (PBS) ternary phase with a molar ratio of 40:40:20 was selected. Tri-n-butyl borate ($C_{12}H_{27}BO_3$ 98+%, International Lab, USA) was used as the boron compound while tetraethoxysilane (TEOS 98%, International Lab, USA) was used as the Si source. Solution formed by dissolving Pb $(CH_3COO)_2{\cdot}3H_2O$ in 2-methoxyethanol was added to a mixture of TEOS, tri-n-butyl borate, 2-methoxyethanol and deionized water. The molar ratio of TEOS:2-methoxyethanol:deionized water was fixed at 1:4:2. The mixture was then stirred for 2 h at room temperature. The concentration of the PBS solution was adjusted to 1 M by the solvent ethanol. The final solution was then poured into glass vessel and covered for 3 days at room temperature to form a gel. The translucent gel was dried at a temperature of 120°C for 10 h for further processes.

In this modified hybrid process, instead of using PBS glass precursor sol, the nano-sized PZT powders were dispersed into the PBS glass dried gel dissolved in ethanol, and then mixed thoroughly to form PZT(53/47)–PBS powder-solution suspension/slurry by conventional ball milling for 2 h. The mass ratio of the PBS dried gel powders (denoted as gel content/addition) to the nano-sized PZT(53/47) powders is defined as:

$$W_{gel}(wt\%) = \frac{W_{gel}}{W_{PZT(53/47)}} \times 100\% \quad (1)$$

where W_{gel} and $W_{PZT(53/47)}$ are the weight of PBS dried gel powders and PZT(53/47) powders, respectively. In the present study, glass-ceramic composites with $W_{gel}(wt\%)$

varied between 3 wt.% and 30 wt.% were investigated. The as-prepared uniformly distributed PZT(53/47)–PBS slurry was dried at 120°C, calcined at 450°C for 2 h, and granulated to obtain PZT–PBS ceramic powders. The powders were uniaxially pressed into disk pellets with a diameter of 13 mm and a thickness of about 0.7–1 mm at a pressure of 4 MPa in a stainless steel die. Notice that all the pressed pellets were sintered at 900°C except for 30 wt.% at 850°C for 4 h in air atmosphere.[1]

2.2 Property measurements with characterization

The room-temperature X-ray diffraction (XRD) patterns of the PZT(53/47)–PBS glass-ceramics and nano-sized PZT (53/47) powders calcined at 800°C were investigated using an X-ray diffractrometer (Philips X'Pert-Pro MPD) with Cu $K_{\alpha 1}$ radiation (1.5406 Å, 40 kV, 30 mA) from 2θ=15° to 70°(θ is the diffraction angle) with a scanning step of 0.05° per second, and the intensity was calculated by the APD Philips program. The morphologies of the bulk samples and powders were examined by means of a Scanning Electron Microscope (SEM, JEOL Model JSM-6490). The element analysis was performed by using energy dispersive X-ray spectroscopy (EDX, Oxford/Inca, Energy 250) during the SEM measurements. The apparent densities of all the bulk samples were evaluated by the Archimedes' method.

To study the electrical and piezoelectric behaviors, low temperature fire-on silver paste was applied onto both sides of the glass-ceramics, and heat-treated in air at 600°C for 30 min to form silver electrodes. The temperature dependence of relative permittivity and loss tangent at various frequencies was investigated at a heating rate of 2°C/min using a computer-controlled automated system formed by a precision impedance analyzer (Agilent 4292A), a temperature-controlled furnace (Carbolic) and a multimeter (Keithley 2000). The room-temperature polarization-electric field hysteresis loops were evaluated using a modified Sawyer Tower circuit operated at a frequency of 100 Hz.

3 Results and discussion

3.1 Structural characterization

For the glass ternary system as shown in Fig. 1(a), the XRD investigation shows that the amorphous nature of the PBS dried gel powders. In Fig. 1(b), for nano-sized PZT powders calcined at 800°C, the XRD pattern exhibits a

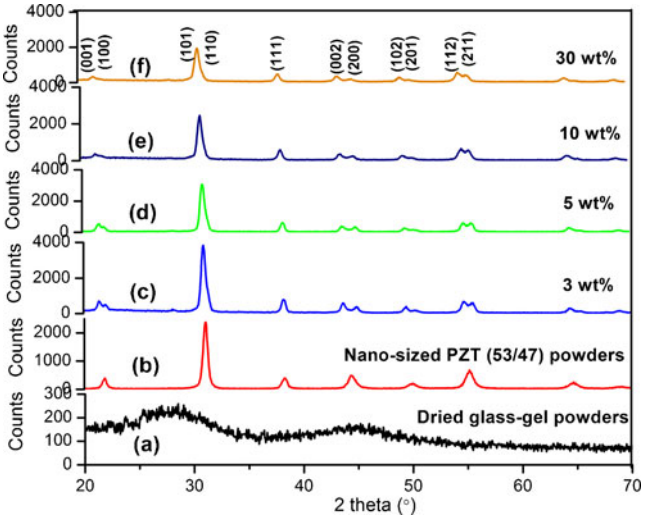

Fig. 1 XRD patterns of PBS gel powders (**a**) dried at 120°C; (**b**) nano-sized PZT(53/47) powders calcined at 800°C, together with (**c**)–(**f**) the glass-ceramic composites with different glass-gel additions

pure perovskite structure. Similarly, the XRD patterns in Fig. 1(c–f) indicate the presence of highly pure and crystalline pervoskite structure in the PZT(53/47)–PBS glass-ceramics. Obviously, all the obtained PZT(53/47) phases are in tetragonal phase. All the peaks are identified with no detection of intermediate or interfacial phases even for the ceramic with 30 wt.% PBS gel content, indicating the success in synthesizing PZT(53/47)–PBS composite ceramics using the modified hybrid processing route. Unsurprisingly, with increasing wt% of glass gel content, the peak intensities of the PZT are slightly diminished.

Since it is well known that the particle size is an important issue in perovskite ceramics, the crystalline structure of nano-sized PZT(53/47) powders calcined at 800°C was investigated carefully in Fig. 2. The SEM micrograph reveals that most of the crystalline particles are round with uniform crystallite size of 70–160 nm using the Feret's diameter. However, few rectangle crystalline particles about 600 nm in size are observed.

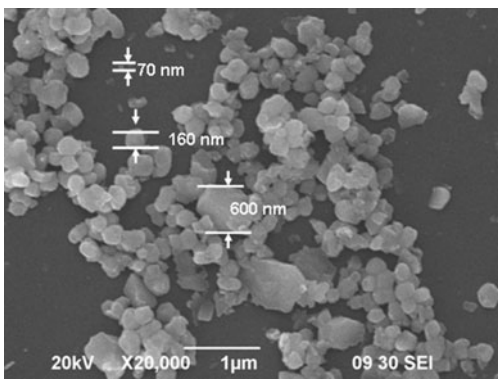

Fig. 2 The SEM micrograph of nano-sized PZT(53/47) powders

[1] All the selected samples for structure and property measurements are the same as above sintering temperatures.

The surface morphologies of the glass-ceramic samples of different PBS gel contents are illustrated in Fig. 3(a–h), together the cross-sectional micrographic picture of a typical sample with 5 wt.% glass gel and EDS analyses at two spots are shown in Fig. 3(i), respectively. As shown in Fig. 3(a–h), generally speaking, dense, homogeneous, and well-developed microstructures are obtained at low-firing temperature. One can clearly observe that the grain sizes of PZT(53/47) phases (about 1–2 μm in size) are quite uniform in the samples with no large grain observed. The results denote that agglomeration, which easily occurs in conventional sol–gel derived glass-ceramics, could be overcome by this modified hybrid process, demonstrating the advantage of this novel route. For the samples with 3–7 wt.% glass-gel content, the relative density is about 94% TD (theoretical density), and in 10–30 wt.% samples, the relative density is about 91% TD. The reasons may be caused by the increase of defects, such as pores, interfaces and grain boundaries, with increasing wt% glass-gel content. However, as far as the fine-grained glass-ceramic composite is concerned, it is a relatively dense (>70% TD) composite.

In Fig. 3(i), the image exhibits a mixture of intergranular and transgranular feature in the glass phase, indicating that grains and boundaries have approximately same strength. EDS analysis indicated that the measured composition of the crystal is generally close to the expected composition of PZT i.e. Pb : Zr+Ti ≈ 1 : 1. Also, the Zr : Ti ratio is slightly lower at the grain boundary region (mark 1) than at the bulk (mark 2).

As seen from Fig. 3, the PBS gel solution acted as binding agent to connect the PZT(53/47) particles and filled the interstitials of the PZT(53/47) particles. This is one of the advantages of hybrid process which easily achieves dramatic modification of the processing behaviors of ceramics. This process can produce uniform, fine-grained and high-quality ceramics at low sintering temperatures. On one hand, it combines the merits of high crystallinity and high performance of nanocrystalline particles with those of low sintering temperature due to the sol–gel wet chemistry process as above mentioned. On the other hand, it reduces the particle-to-particle interaction for better processing nanoparticles. It is understandable that there is no agglomeration phenomena observed and the homogeneous microstructure obtained, as well as the presence of glass only dispersed at grain boundaries as glassy matrix. This is one of the features of this novel hybrid process. Moreover, the modified hybrid process proposed in this experiment (i.e., gel solution in place of the sol precursor) can concisely control the amount of the crystalline phase content employed in the matrix, which provides an easy, flexible, and reproducible feature in synthesizing different ferroelectric and composite ceramics.

3.2 Dielectric properties

The variation of dielectric constant with temperature for a typical 5 wt.% sample measured at 1 kHz–1 MHz is shown in Fig. 4(a), and the variations of dielectric constant with temperature at 10 kHz for the samples with 3–10 wt.% of glass gel contents are displayed in Fig. 4(b), respectively. Inset shows the loss tangent as a function of temperature. As shown in Fig. 4(a), the room-temperature dielectric constant and loss tangent are found to be 920 and 0.02, respectively at 1 kHz. Also, the dielectric constant of PZT(53/47)–PBS glass-ceramic peaks at different temperatures and frequencies, which shows that the dielectric constant of PZT(53/47) crystals surrounded by a glassy matrix has the characteristic dispersion at the Curie point. This indicates that the glass-ceramic composite has a strong tendency of diffusion phase transition. This may be ascribed to the finer structure and the glass-ceramics containing $PbO\text{-}B_2O_3\text{-}SiO_2$ continuous matrix, resulting in a diffused peak.

Additionally, as seen from Fig. 4(a), the dielectric constant of the sample at T_c (about 400°C) does not drop with increasing temperature at 1 kHz; however, at high frequency of 1 MHz, the decrease in dielectric constant at high temperature is more evident. The apparent increase in dielectric constant at elevated temperature is due to increase loss in this temperature range, as shown in the inset of the figure. This trend is consistent with the act that PZT crystals surrounded by a glassy matrix have a higher electrical conductivity at higher temperature. In amorphous materials, the ease of polarizability, and hence dielectric constant, increases with temperature because of their relatively weak bonding structure. In Fig. 4(b), with increasing glass gel content, the maxima in these plots are broader. Their T_c values shift towards higher temperature side confirming the diffused phase transition. In general, the greater the wt% of glass gel content, the lower is the peak value of dielectric constant due to residual glass phase which have lower dielectric constant compared to PZT(53/47) phase. But for the samples with high wt% of glass gel content (e.g. 7 and 10 wt.%), the dielectric constant increases apparently above the Curie temperature owing to the increased loss as shown in the inset of Fig. 4(b). The results illustrate that the fine-grained PZT (53/47) based glass-ceramic composites presented in this work have higher electrical conductivity at higher temperature with increasing glass gel content.

We try to find the relationship between the theoretical predictions and experimental values of the room-temperature effective dielectric constant at 1 kHz. Figure 5 shows the comparison of the composites dielectric constant with the experimental data. In the present work, because the glass-ceramics prepared by

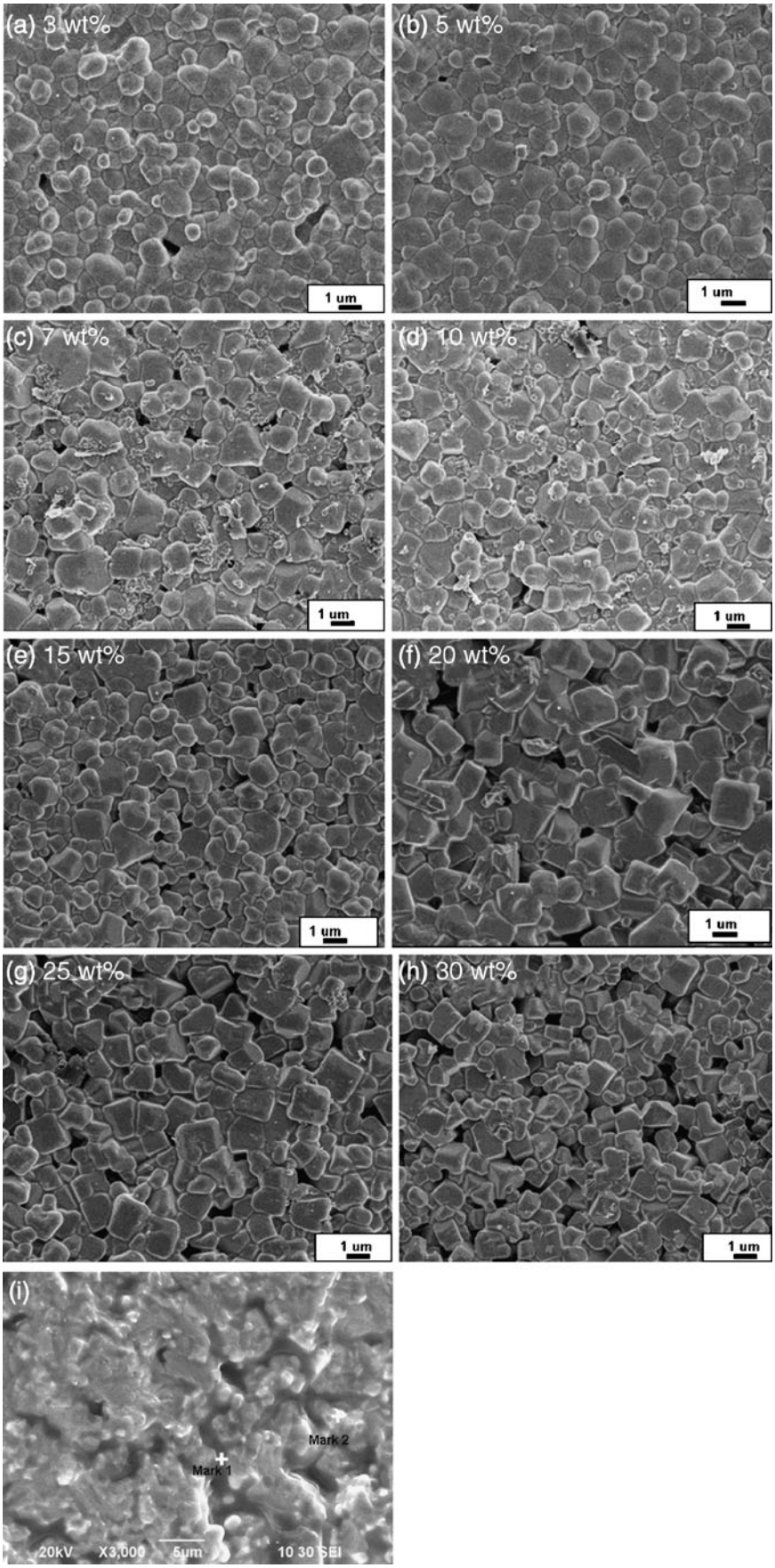

Fig. 3 Nature surface images of glass-ceramic composites with various amount of glass-gel addition under air atmosphere: (**a**) 3; (**b**) 5; (**c**) 7; (**d**) 10; (**e**) 15; (**f**) 20; (**g**) 25; and (**h**) 30 wt.%; (**i**) Fracture morphology of a typical sample with 5 wt.% glass-gel content, together with EDS analyses at two spots

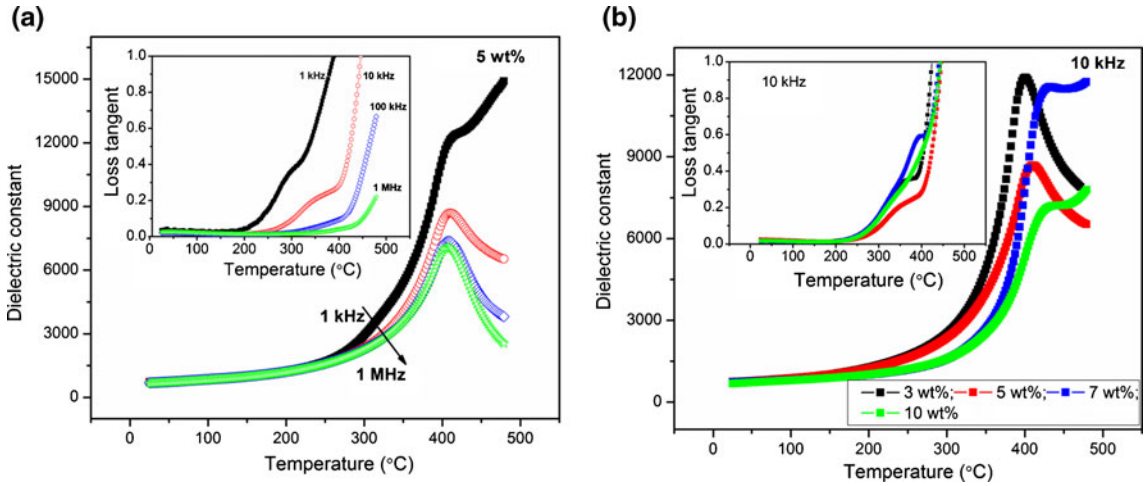

Fig. 4 (**a**) Temperature dependent dielectric constant for a typical 5 wt.% sample at 1 kHz–1 MHz; (**b**) glass-ceramic composites with 3–10 wt.% at 10 kHz. Insets show the corresponding temperature dependent loss tangent

modified hybrid process consist of a PBS glass gel phase having a relatively low dielectric constant and a nano-sized PZT(53/47) powder phase having high dielectric constant, the glass-ceramic composites can be generally considered as a 0–3 connected composite. Poon et. al.'s model [25] is a good prediction for most situations applicable to the whole range of the volume fraction of the inclusions (i.e. PZT(53/47)), assuming that each phase is uniform and has the same properties throughout the composite, and the third phase in the composite (such as grain boundaries, interface and pores) is neglected. Consider a particulate-filled composite material composed of dielectric spheres (inclusions) with dielectric constant ε_i dispersed in a continuum medium (matrix) with dielectric constant ε_m. Therefore, the effective dielectric constant of the composite (ε) is found by using Eq. (2):

$$\frac{\varepsilon}{\varepsilon_m} = 1 + \frac{\phi\left(\frac{\varepsilon_i}{\varepsilon_m} - 1\right)}{\phi + \frac{1}{3}(1-\phi)\left[\frac{\varepsilon_i}{\varepsilon_m}(1-\phi) + \phi + 2\right]} \tag{2}$$

where ε_i and ε_m are the dielectric constants of the inclusion and the matrix respectively, and ϕ is the volume fraction of the inclusions (defined as the volume of the inclusion divided by the volume of all constituents of the mixture sintered at 850–900°C). The theoretical densities of the PBS glass [26] and PZT (53/47) from nano-sized PZT powder (Fig. 1(b)) are 5.33 g/cm^3 and 8.03 g/cm^3, respectively. The percentage of PBS gel-content weight loss from 25 to 900°C determined by the TG curve (not shown) is approximated to be 80. For the various $W_{gel}(wt\%)$ of 3, 5, 7, 10, 15, 20, 25, and 30 wt.% samples, the corresponding volume fractions of the matrix are 0.79, 1.13, 2.10, 2.50, 4.34, 5.70, 7.02, 8.31%, respectively. The dielectric constants for the fine PZT (ε_i) [27] and glass matrix (ε_m) [28] were 1,240 and 19, respectively.

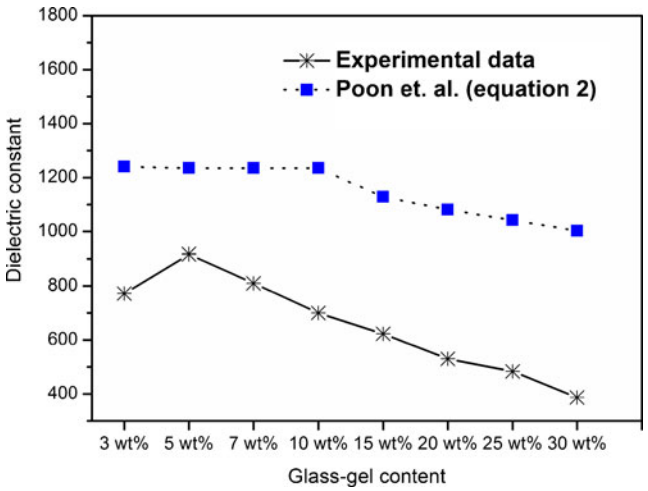

Fig. 5 Comparison of the effective dielectric constants of glass-ceramic composite obtained from experiments and Eq. 2

As one can see, for the effective dielectric constant, the values of the actual experimental data are far from the predictions, showing a larger derivation at high volume fraction of glass content. One is the grain-size structure which can affect ferroelectric properties; the other is the limitation of the equation at high volume fraction of the inclusion. Moreover, there are some other reasons as follows: (1) the predictions are based on the assumption that the third phase (i.e. grain boundaries, interface or pores) has no impact on the characteristics of the glass-ceramics composites. However, with increasing wt% glass gel content, the increases of the interfaces and pores with

low dielectric constant can reduce the effective dielectric constant. On the other hand, the grain boundaries and pores will contribute to additional pinning points for the moving domain walls resulting in a low dielectric constant; (2) the grain boundaries cause space charges at the interface between the inclusion and the matrix, leading to some degree of depolarization and hence decrease the dielectric constant.

3.3 Ferroelectric properties

Figure 6 shows the polarization-field hysteresis loops ($P-E$) of the samples with 3, 5, 7, 10, 15 and 30 wt.% glass-gel contents. These hysteresis loops show reasonable ferroelectricity of PZT(53/47) crystallites derived from the modified hybrid process. It is obvious that a high volume fraction of the ferroelectric PZT(53/47) phase exists in these samples in spite of containing higher wt% glass-gel contents. It is noticed that the $P-E$ loops shift slightly to the right, presumably caused by the space charge occurring in the samples at low frequency (100 Hz), for there are grain boundaries existed in the glassy phase. Among the polarization curves, the electric field excursion is higher for the 5% than for the other glass loadings. This might be due to the variation in the samples' porosity. Corresponding to Fig. 6(a–f), the best ferroelectric property is obtained in the 5 wt.% sample, the values of P_s, P_r and E_c are 21.9 μC/cm^2, 10.8 μC/cm^2 and 2.19 kV/mm, respectively. These values are smaller than those obtained from commercial soft PZT [29] which has the corresponding values of 39 μC/cm^2, 26 μC/cm^2 and 7.8 kV/mm. On the basis of our results, we demonstrate that these fine-grained ferroelectric glass-ceramic composites have great potential for micro electronic component applications.

4 Conclusion

A modified hybrid process has been successfully introduced to prepare well-sintered and fine-grained ferroelectric $Pb(Zr_{0.53}Ti_{0.47})$–based glass-ceramics with dense and uniform microstructures at low sintering temperatures of 850–900°C. The temperature dependence of the dielectric constant of PZT based glass-ceramics revealed that the glass has a higher electrical conductivity in the range of higher temperature. Well-defined ferroelectric hysteresis loops ($P-E$) are observed due to the high volume fraction of the well-crystalline PZT(53/47) phase content. Predica-

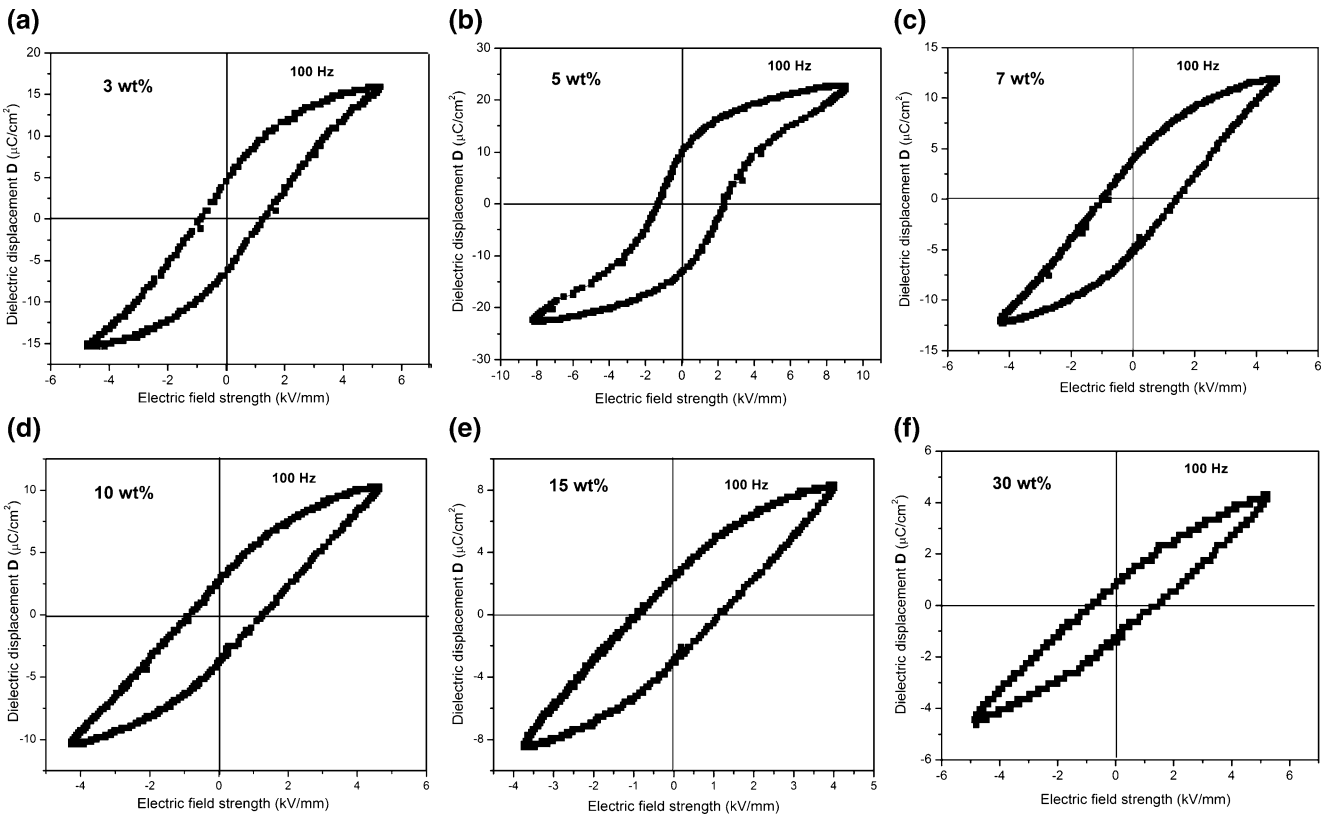

Fig. 6 Ferroelectric hysteresis loops of glass-ceramic composites with various wt% glass-gel contents: (**a**) 3; (**b**) 5; (**c**) 7, (**d**) 10; and (**e**) 15 and (**f**) 30 wt.%

tions showing deviations from the experimental data could be attributed to the effects of the finer structure and the existence of third phases such as grain boundaries, interfaces and pores. Although the modified hybrid process is proposed for fabricating glass-ceramics, in fact, we consider that this simple, flexible and reproducible approach should also be useful for almost all ceramic processes, realizing the dream of retaining a fine or ultra-fine grain size in fully sintered products at relatively low firing temperature.

Acknowledgements This work was supported by the Hong Kong Polytechnic University under Grant No. GU-694. The authors would like to thank Dr. S.W. Or and Prof. Helen Chan for their helpful discussions.

References

1. J. Collier, I.A. Cornejo, M.J. Haun, Ferroelectrics **154**, 47–52 (1994)
2. H.D. Chen, K.R. Udayakumar, L.E. Cross, J.J. Berstein, L.C. Niles, J. Appl. Phys. **77**, 3349–3353 (1995)
3. R. Mass, M. Koch, N.R. Harris, N.M. White, A.G.R. Evans, Mater. Lett. **31**, 109–112 (1997)
4. B. Morten, G.D. Cicco, M. Prudenziati, Sensor Actuator A **31**, 153–158 (1992)
5. H. Moilanen, S. Leppävuori, Microelectron. Int. **37**, 28–30 (1995)
6. D.R. Ulrich, Solid State Tech. **12**, 30–31 (1969)
7. M.S. Multani, S.G. Gokarn, R. Vijayaraghavan, V.R. Palkar, Ferroelectrics **37**, 652 (1981)
8. W. Chaisan, S. Ananta, T. Tunkasiri, Curr. Appl. Phys. **4**, 182–185 (2004)
9. E.R. Nielsen, E. Ringgarrd, M. Kosec, J. Eur. Ceram. Soc. **22**, 1847–1855 (2002)
10. M. Yasuoka, T. Shirai, K. Watari, J. Therm. Anal. Calorim. **93**, 59–62 (2008)
11. K.R. Chowdary, E.C. Subbarao, Ferroelectrics **37**, 689–692 (1981)
12. O. Parkash, D. Kumar, L. Pandey, Bull. Mater. Sci. **8**, 557–565 (1986)
13. M.M. Layton, A. Herczog, Glass Technol. **10**, 50–53 (1969)
14. T. Kokubo, M. Tashiro, J. Non-Cryst. Solids **13**, 328–340 (1973)
15. G.H. Beall, B. Flats, L.R. Pinckney, US Patent No. 5,491,116, February 13, (1996)
16. K. Yao, L.Y. Zhang, X. Yao, W.G. Zhu, J. Am. Ceram. Soc. **81**, 1571–1576 (1998)
17. J.W. Zhai, X. Yao, L.Y. Zhang, J. Electroceram. **5**, 211–216 (2000)
18. K. Saegusa, Jpn. J. Appl. Phys. **36**, 3602–3608 (1997)
19. K. Yao, L.Y. Zhang, X. Yao, J. Mater. Soc. **32**, 3659–3665 (1997)
20. H. Dislich, J. Non-Cryst. Solids **80**, 115–121 (1986)
21. H.F. Zhang, X. Yao, L.Y. Zhang, J. Am. Ceram. Soc. **90**, 2333–2339 (2007)
22. H.F. Zhang, S.W. Or, H.L.W. Chan, J. Appl. Phys. **104**, 104109 (2008)
23. H.F. Zhang, S.W. Or, H.L.W. Chan, K.W. Kwok, J. Phys. Chem. Solid **70**, 1218–1222 (2009)
24. H.F. Zhang, S.W. Or, H.L.W. Chan, F. Yang, J. Eur. Ceram. Soc. **31**, 1753–1761 (2011)
25. Y.M. Poon, F.G. Shin, J. Mater. Sci. **39**, 1277–1281 (2004)
26. S. Fujino, C. Hwang, K. Morinagat, J. Am. Ceram. Soc. **87**, 10–16 (2004)
27. H.T. Martirenat, J.C. Burfoot, J. Phys. C Solid State Phys. **7**, 3182–3192 (1974)
28. Z.D. Guan, Z.T. Zhang, J.S. Jiao (eds.), *The physics of inorganic materials* (Tsinghua University Publisher, Tsinghua, 1992), p. 317
29. R. Yimnirun, Y. Laosiritaworn, S. Wongsaenmai, J. Phys. D Appl. Phys. **39**, 759–764 (2006)